AJNR

Ultrafast Diffusion-Sensitive MR Imaging of Brain on an Open Scanner at 0.2 T

Fritz Schick, Thomas Nägele, Dirk Wildgruber, Jochen Trübenbach and Claus D. Claussen

AJNR Am J Neuroradiol 1999, 20 (1) 53-61
http://www.ajnr.org/content/20/1/53

AJNR Am J Neuroradiol 20:53–61, January 1999

Technical Note

Ultrafast Diffusion-Sensitive MR Imaging of Brain on an Open Scanner at 0.2 T

Fritz Schick, Thomas Nägele, Dirk Wildgruber, Jochen Trübenbach, and Claus D. Claussen

Summary: We describe new strategies for fast diffusion-sensitive MR imaging of ischemic brain or spinal cord lesions. The methods provide diagnostic image quality in less than 1 s per section and are used in conjunction with low-field-strength open MR scanners. Single-shot sequences combine diffusion-sensitive preparation with a modified fast spin-echo data acquisition. Results are presented from healthy volunteers and from two patients with recent and older ischemic brain lesions.

Diffusion-weighted MR imaging has proved to be of great value in early detection of ischemic brain lesions. Animal studies (1–3) and examinations in patients with neurologic disorders (4–6) have been conducted using several MR diffusion-weighted imaging techniques. The results show that diffusion-weighted imaging allows early detection of the ischemic areas several hours before conventional relaxation characteristics change. Furthermore, the age of an ischemic lesion visible on standard T1- and T2-weighted images can be estimated using the diffusion-weighted imaging technique (5–7). Ischemic parenchymal lesions have a clearly decreased apparent diffusion coefficient (ADC) only in the early phase, lasting several days, whereas older lesions show nearly normal behavior or increased ADC values on diffusion-weighted images. Other MR imaging techniques are less capable of distinguishing ischemic lesions of different ages, which are frequently present in stroke patients.

Although diffusion-weighted imaging is a promising method in diagnostic imaging of ischemic stroke, its successful application in patients has been difficult, owing to practical limitations. Diffusion-weighted spin-echo sequences with navigator echoes for phase correction (6, 8, 9) provide excellent results in phantoms and in motionless volunteers. Major drawbacks of this approach are the very long measuring time of several minutes and the unsatisfactory results obtained in patients unable to remain still during the examination. In principle, diffusion imaging on open MR systems with low field strength is possible, although the method has more frequently been implemented at high field strength.

A clearly faster alternative to these spin-echo techniques is diffusion-prepared echo-planar imaging (EPI) sequences (7, 10). A complete diffusion-weighted image of good quality can be acquired in about 200 msec by EPI (11), but high sensitivity to inhomogeneities of the magnetic field must be considered. Geometric and intensity distortions are induced by susceptibility changes between different anatomic regions and by inhomogeneities of the applied magnetic field. In addition, frequency-selective water excitation or fat saturation must be applied to avoid artifacts. Therefore, EPI is more practicable on closed magnets, which provide good homogeneity of the magnetic field. In diffusion-sensitive applications of EPI, further distortions caused by eddy currents after diffusion-sensitizing gradients occur (12).

In this article, we describe a rapid diffusion-sensitive imaging technique with a minimum measuring time of about 0.5 s, which provides diagnostic diffusion-weighted images even on an open MR imaging system at low field strength.

Methods

A spin-echo signal becomes sensitive to diffusion (random molecular motion) using a long-duration high-field gradient with the same integral $\int G\,dt$ (G is the gradient $\partial B/\partial r$) applied before and after the 180° refocusing pulse (13) as shown in Figure 1A. Diffusion leads to a loss in the amplitude of the recorded signals. The gradient system of our open MR scanner (Magnetom Open, Siemens, Erlangen, Germany) allows a slew rate of 0.6 msec from 0 to maximal 15 mT/m along each axis for short total durations of up to 5 msec. On the other hand, the maximum gradient amplitude for diffusion-sensitizing gradients with long duration is only about 13.8 mT/m (all three gradient channels have to be switched simultaneously). Thus, b values of 500 s/mm^2 (1000 s/mm^2) could be obtained after a preparation time of about 80 msec (100 msec).

Usual fast spin-echo imaging with recording of several echoes refocused by RF pulses after one 90° excitation has been shown to provide similar image quality relative to standard spin-echo techniques, but with markedly shorter measuring times (14). A reduction of the measuring time in diffusion-weighted spin-echo imaging is also possible using a fast spin-echo approach; however, a modified data acquisition strategy

Received October 7, 1997; accepted after revision April 6, 1998.

Supported by a grant from the Federal Ministry of Education and Research and the Interdisciplinary Clinical Research Center (IKFZ), Tübingen, Germany.

From the Departments of Diagnostic Radiology (F.S., J.T., C.D.C.), Neuroradiology (T.N.), and Neurology (D.W.), University of Tübingen, Germany.

Address reprint requests to Priv.-Doz. Dr. Dr. Fritz Schick, Radiologische Klinik, Abteilung für Radiologische Diagnostik, Hoppe-Seyler-Str. 3, 72076 Tübingen, Germany.

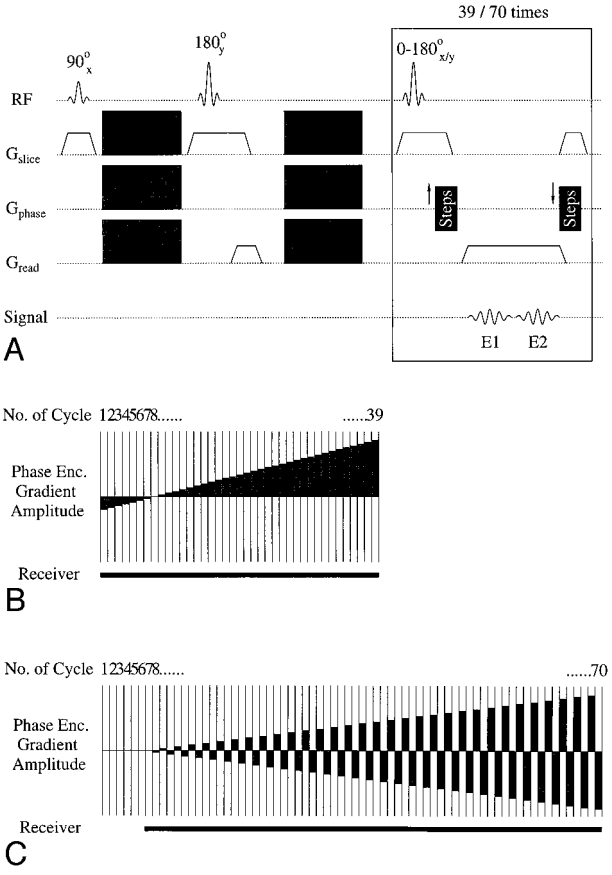

FIG 1. Single-shot diffusion-weighted imaging with the SPLICE acquisition technique.

A, Sequence of RF pulses and magnetic field gradients. Diffusion weighting is achieved by a spin-echo preparation with strong gradients applied before and after the 180° refocusing pulse. The modified fast spin-echo train with two families of signals (E1 and E2) is generated by repetition of the elements inside the box. Two complete magnitude images from echo trains E1 and E2, respectively, should be added to obtain the final image with higher SNR.

B, Phase-encoding steps for half-Fourier reconstruction from the signals in echo train E1 and E2, respectively. Sixty-four lines in the final image are considered in the given example.

C, Phase encoding with centric reordering of the steps for an acquisition of a complete raw data matrix with 64 steps. Data recording starts after six cycles in the fast spin-echo train. This delay allows the spin system to reach an equilibrium state with similar signal intensities in both echo families E1 and E2.

must be applied (15–17). Figure 1A shows a complete single-shot fast spin-echo sequence with diffusion preparation and two separated echo trains, E1 and E2. The fast spin-echo refocusing is repeated for sampling a complete set of raw data for one image from echoes E1 and one image from echoes E2, respectively. The final image is an addition of both single-magnitude images reconstructed from two separate raw data sets.

Several phase-encoding strategies potentially lead to relatively short TEs for the central lines in the k-space and minimum artifacts from the signal decay during acquisition. Figure 1B shows the phase-encoding steps for half-Fourier acquisition. The Margosian partial Fourier approach (18) with phase correction and a real display of the reconstruction was applied. Both echo families (E1 and E2 in Fig 1A) are recorded with the same phase encoding in a given cycle of the modified fast spin-echo train. The signal amplitudes in E1 and E2 are clearly different and fluctuating in the first steps, but they become very similar and regular after about six periods in the train. The reconstruction shows only slight sensitivity to the signal behavior in the first steps, mainly used for phase correction. An acquisition of the central Fourier lines in the eighth step of the modified fast spin-echo train (Fig 1B) leads to acceptable quality in the single images from echoes E1 and E2 and in the final image. The reconstruction was performed without magnitude normalization of the raw data.

A further approach to suitable single-shot data recording is the use of centric reordering of the phase-encoding steps, as shown in Figure 1C. This strategy leads to data for filling the entire k-space. As described above, about six cycles of fast spin-echo refocusing are necessary to obtain an equilibrium between both echo families (E1 and E2). Thus, recording of data is started after these precycles, beginning with the central Fourier line. In this approach, the signal-to-noise ratio (SNR) in species with long relaxation times, T2, is improved relative to the half-Fourier acquisition, and some problems with artifacts associated with the required phase relations of signals in the half-Fourier acquisition can be avoided. On the other hand, the fast spin-echo train is clearly prolonged as compared with Figure 1B, and the time interval between consecutive phase-encoding steps is doubled.

Parameters of the described techniques had to be optimized to obtain acceptable results on a 0.2-T open MR scanner. The optimization was performed using phantoms containing $MnCl_2$-doped water with concentrations between 0.2 mM and 0.5 mM and by human brain examinations in healthy volunteers. The subjective criteria in the optimization were high SNR and avoidance of blurring artifacts on the images. The timing of the fast spin-echo train is mainly determined by the readout time for the echoes E1 and E2 and by the required spatial resolution, with the minimum field of view (FOV) about 150 × 300 mm for a 96 × 256 matrix. Long readout times lead to improved SNR from species with a long T2 in the images, but increased blurring artifacts due to transverse relaxation during data recording must be accepted from species with a short T2. The latter problem can be partly solved by using reduced flip angles of the refocusing pulses, because stimulated echo contributions with reduced losses of magnetization are more pronounced. However, the absolute signal amplitude is reduced in this case. Sequences providing a good compromise between SNR and blurring effects were applied for clinical examinations (see Table). The readout period for each echo (E1 and E2) was 2.56 msec, and one cycle of the fast spin-echo acquisition had a duration of 7.1 msec. Thus, the recording time for half-Fourier acquisition was about 280 msec for a 64 × 256 matrix using half-Fourier acquisition (Fig 1B), but nearly 500 msec in the approach with centric reordering. The recording time is relatively long with respect to the relaxation times in brain at 0.2 T (T1 = 600 and T2 = 100 in gray matter, T1 = 350 and T2 = 90 in white matter, T1 ≈ 2.5 s and T2 ≈ 800 in CSF). Ischemic lesions show clearly longer transverse relaxation times than normal brain several days after onset. Numerically optimized refocusing pulses similar to Hanning-filtered sinc pulses with one side lobe were provided by the manufacturer and applied for section-selective refocusing in the echo train. The flip angles of the pulses with a duration of 1.0 msec were set to a nominal 150° (ie, the flip angle in the center of the section) in the half-Fourier sequences and to a nominal 120° using centric reordering of the phase-encoding steps. The nominal flip angles for the centric reordering approach were lower, since the echo train is clearly longer in this case compared with half-Fourier encoding. The lower flip angle leads to a decreased signal intensity at the beginning of the echo train, but the signal decay is less pronounced owing to the contributions from stimulated echoes (14).

Results

Single-shot diffusion-prepared sequences with half-Fourier acquisition (Fig 1B) or with centric reordering of the phase-encoding steps (Fig 1C) were applied using various *b* values for an assessment of

Suitable parameters of sequences with half-Fourier reconstruction versus centric reordering of phase-encoding for brain diffusion imaging at 0.2 T

Parameter	Half-Fourier	Centric Reordering
Matrix size	64–96 × 256	64–96 × 256
Number of phase-encoding steps	39–59	64–96 (+ 6 precycles)
Nominal refocusing angle in the echo train	≈ 150°	≈ 120°
Period of refocusing in the echo train	7.10 msec	7.10 msec
Readout time for each echo	2.56 msec	2.56 msec
Field of view for single-shot images	225–250 mm × 450–500 mm	200–250 mm × 400–500 mm
Section thickness for single-shot images	12–15 mm	≈ 12 mm
Field of view for averaged images (10 scans)	160–180 mm × 320–360 mm	150–180 mm × 300–360 mm
Section thickness for averaged images (10 scans)	10–12 mm	≈ 10 mm
Minimum TE for $b = 100$ s/mm^2	104 msec	97 msec
Minimum TE for $b = 250$ s/mm^2	119 msec	112 msec
Minimum TE for $b = 500$ s/mm^2	135 msec	128 msec
Minimum TE for $b = 1000$ s/mm^2	155 msec	148 msec
Minimum TE for $b = 2000$ s/mm^2	180 msec	173 msec

Note.—The given rectangular fields of view are suitable if 256 sample points are used in readout direction. Similar results are expected using a quadratic field of view (eg, 175 × 175 mm instead of 175 × 350 mm) and a readout resolution of 128 points. However, the rectangular approach avoids cut-off problems in readout direction. The minimum TEs are based on a spin-echo diffusion preparation and a maximal gradient amplitude of 13.8 mT/m.

brain regions with altered diffusion. The value of b can be calculated from the gradient amplitude, A, the gradient duration, δ, and the interval, Δ, by $b = (\gamma \times A \times \delta)^2 \times (\Delta - \delta/3)$. Constant γ in the equation represents the gyromagnetic ratio of protons: $\gamma = 2.675 \times 10^8$ 1/Ts. The minimum TEs on our imager using spin-echo diffusion preparation are reported in the Table.

The differences in the image quality between various methodical approaches were assessed in examinations of five healthy volunteers. Figure 2 shows transverse images recorded from a 36-year-old male subject. The images in Figure 2A and B were obtained by the half-Fourier approach with 96 lines in k-space (55 lines were recorded, the eighth one is the central line in k-space). Both images were recorded using an unchanged timing scheme, and the duration between the 90° excitation and the recording of the central line in k-space (called TE in the following text) was 155 msec. For the image in Figure 2A, the amplitude of the diffusion gradient was set to zero, whereas Figure 2B was recorded after diffusion sensitizing with a b value of 1000 s/mm^2. The effects of the diffusion weighting without signals from free water protons are well demonstrated. Each image was acquired in 500 msec. The half-Fourier echo train required about 400 msec for signal recording. In contrast, the images in Figure 2C and D stem from a sequence with 96 phase-encoding steps for the entire k-space using the centric reordering scheme (Fig 1C, with six refocusing cycles without signal recording before scanning the central line in k-space in the seventh cycle). Again, an unchanged timing scheme was applied for both images. The preparation applied for Figure 2C (without diffusion weighting) corresponds to Figure 2A, whereas Figure 2D was obtained using a diffusion preparation with $b = 1000$ s/mm^2, as applied for Figure 2B. The TE for Figure 2C and D was 148 msec, the measuring time for each image was 840 msec, and the echo train had a duration of 690 msec. A comparison between Figure 2A and B and Figure 2C and D shows that the half-Fourier approach provides sharper contours in the images and less blurring artifacts along the phase-encode direction (from left to right). On the other hand, the SNR of brain is better in the images taken with complete k-space sampling and reordered line scanning.

SNR and/or spatial resolution can be improved by repeated measurements of the same section and averaging of the signals in the final magnitude images. Figure 3 shows images obtained with reordered line scanning (Fig 1C) from a 28-year-old volunteer. Each of the images represents the averaged signal from eight single images recorded with unchanged parameters using a TR of 6 s. The TE for each pair of images (3A and B, 3C and D, 3E and F) was chosen to be as short as possible (Fig 3A without diffusion sensitivity and Fig 3B with $b = 250$ s/mm^2: TE = 112; Figure 3C without diffusion sensitivity and Figure 3D with $b = 500$ s/mm^2: TE = 135; Figure 3E without diffusion sensitivity and Figure 3F with $b = 1000$ s/mm^2: TE = 155). The quality is clearly better in the averaged images as compared with the single scans in Figure 2. About 45 s is required for eight single scans to be averaged; however, multisection imaging with seven to 12 sections, depending on the number of phase-encoding steps, can be performed with TRs of 6 s for nearly complete relaxation between consecutive scans. This procedure leads to a set of diffusion-weighted images with good quality in a measuring time of less than 1 minute on an open scanner. All images in the presented example were recorded without ECG triggering. All single images were of very similar quality. This finding indicates that the method is unaffected by brain or fluid motions throughout the cardiac cycle. Furthermore, test measurements with intentional head rotations

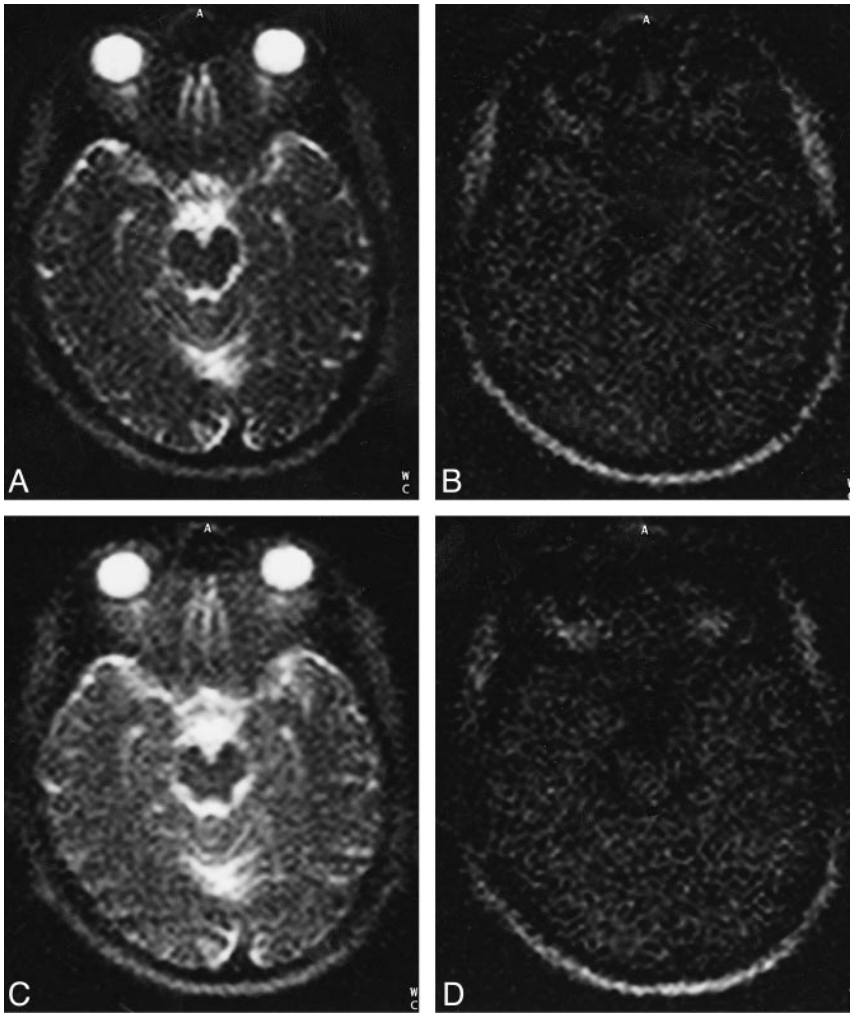

FIG 2. Examples of different types of SPLICE images from the head of a 36-year-old healthy volunteer. Each image, with a 12-mm thickness, was recorded in less than 1 s. The FOV was 210 × 420 mm with a matrix of 96 × 256. *A* and *C* were recorded without diffusion gradients, whereas diffusion sensitizing with b = 1000 s/mm² (maximum amplitude 13.8 mT/m, from 8.0 mT/m in all three orientations simultaneously) was applied for the images in *B* and *D*. The timing scheme in the spin-echo preparation remained unchanged for all images. The images recorded with half-Fourier acquisition (*A, B*) show less blurring artifacts, whereas the SNR is superior in images recorded with centric reordering (*C, D*). The displayed images are magnified and do not show the entire matrix in read direction.

A, Half-Fourier recording as shown in Figure 1B; 55 phase-encoding steps; TE = 155; no diffusion preparation. SNR of brain is 5.5.

B, Half-Fourier technique, with diffusion preparation. SNR of brain is 2.0.

C, Centric reordering as shown in Figure 1C; 96 phase-encoding steps; TE = 148; no diffusion preparation. SNR of brain is 7.3.

D, Centric reordering, with diffusion preparation. SNR of brain is 2.3.

(about 5° per second) showed the method to be very robust in the single scans. On the other hand, the addition of single images to improve the SNR is only useful in scans recorded in a nearly unchanged position.

Results from diffusion-sensitive examinations in patients with ischemic brain lesions are reported below. The images in Figures 4 and 5 show a large ischemic infarction in the territory of the right middle cerebral artery of a 74-year-old patient. All images were recorded 10 days after acute stroke. One coronal single-scan image without (Fig 4A–C) and one with (Fig 4D–F) diffusion weighting (b = 1000 s/mm²) were recorded using the half-Fourier approach with an FOV of 250 × 500 mm for a 96 × 256 matrix. The timing was unchanged in both sequences with a TE of 155, but the amplitude of the diffusion-sensitizing gradient was 0 or 13.8 mT/m, respectively. The addition of the images from echoes E1 (Fig 4A and D) and from echoes E2 (Fig 4B and E) shows a clear signal gain. The combined images (Fig 4C and F) show an increased SNR by a factor of $\sqrt{2}$. The contrast-to-noise ratio (CNR = [signal intensity of lesion − signal intensity of normal brain]/noise) of the lesion in the final diffusion-weighted image (Fig 4F) is equal to 11. Axial sections were recorded using standard fast spin-echo imaging techniques with T1 and T2 weighting (Fig 5A and B). Additional single-scan images with an FOV of 250 × 500 mm and a matrix of 96 × 256 are presented in Figure 5C (TE = 155, without diffusion weighting) and in Figure 5D (TE = 155, b = 1000 s/mm²). In a further study, 20 scans of the same sections were sampled using a TR of 6 s and a reduced FOV of 175 × 350 mm. One series without and one series with diffusion weighting were recorded. The patient clearly rotated his head in the coil during the measurement, as visible in the single images, but 10 images from each series with similar head positions were selected for averaging. The averaged images in Figure 5E and F show an improved spatial resolution and slightly higher CNR (CNR of the lesion is 13 in Fig 5F) compared with the single-shot images in Figure 5C and D (CNR of the lesion is 12 in Fig 5D).

Ischemic brain lesions of different ages were examined in a 58-year old male patient. The patient showed a relatively recent (6-day-old) lesion in the left brain stem due to a cardiogenic embolus in the posterior inferior cerebellar artery, an older (4-

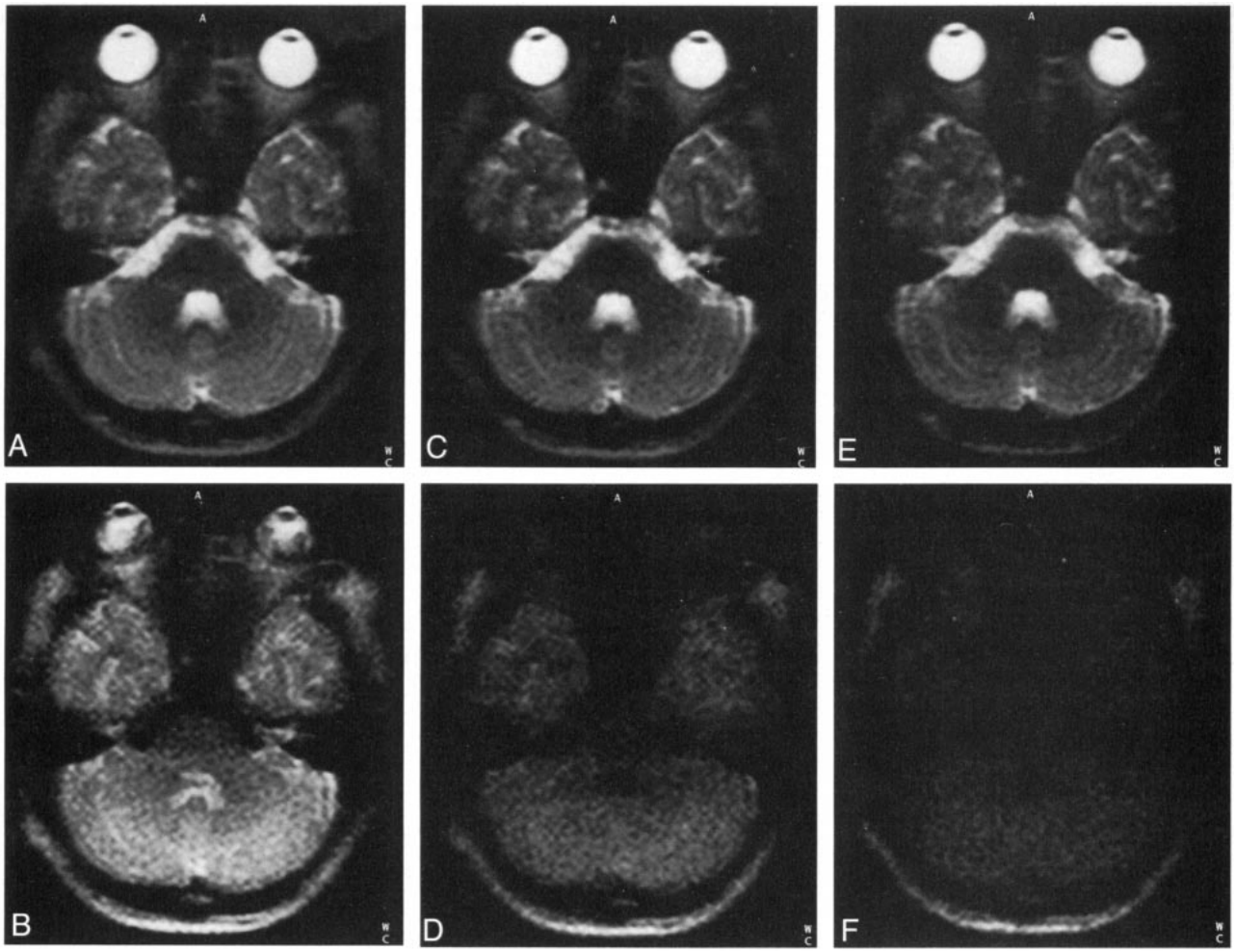

FIG 3. Averaging of several single-shot images allows improved SNR and/or smaller FOV. Averaged transverse sections with a thickness of 10 mm and an FOV of 175 × 350 mm (matrix 96 × 256) from eight single-shot scans in a 28-year-old volunteer. The entire measuring time for one set of images was about 45 s (using a TR of 6 s). Centric reordering and recording of the entire matrix as in Figure 1C were applied.

A, TE = 112; no diffusion sensitivity. SNR of brain is 22.
B, TE = 112; diffusion preparation with a *b* value of 250 s/mm^2. SNR of brain is 15.
C, TE = 128; no diffusion sensitivity.
D, TE = 128; diffusion preparation with a *b* value of 500 s/mm^2.
E, TE = 148; no diffusion sensitivity. SNR of brain is 15.
F, TE = 148; diffusion preparation with a *b* value of 1000 s/mm^2. SNR of brain is 3.3.

week-old) lesion in the mediocaudal part of the right occipital lobe, and a still older (1-year-old) occipitoposterior lesion. Figure 6 exhibits standard T2-weighted fast spin-echo images (Fig 6A, C, and E) of three sections that include the lesions. All lesions appear hyperintense. Single-shot images with diffusion preparation $b = 1000$ s/mm^2 (Fig 6B, D, and F) were recorded using the reported half-Fourier technique. Averaging the signals from eight scans yielded the final images presented in Figure 6. The lesions with different ages can be easily distinguished on the diffusion-weighted images. Only the most recent lesion shows a high signal intensity in Figure 6B, where the CNR of lesion versus normal brain is 10. Figure 6D also reveals decreased diffusion in the 4-week-old lesion, but the signal intensity of the lesion with a CNR of 4 is lower as compared with the early lesion in Figure 6B. The 1-year-old lesion visible in the T2-weighted image in Figure 6E is unremarkable in the corresponding diffusion-weighted image in Figure 6F. Thus, fast diffusion-weighted imaging on the open 0.2-T unit provided further information about the temporal pattern of the focal ischemic lesions in this patient. The reported findings were confirmed by diffusion-weighted EPI on a 1.5-T scanner.

Discussion

We have described new fast imaging techniques that allow diffusion-sensitive single-shot imaging with acceptable SNR on a low-field-strength open MR imager. A modified fast spin-echo acquisition mode, called split acquisition of fast spin-echo signals (SPLICE) (16), was used and optimized for the requirements in diagnostic imaging of ischemic

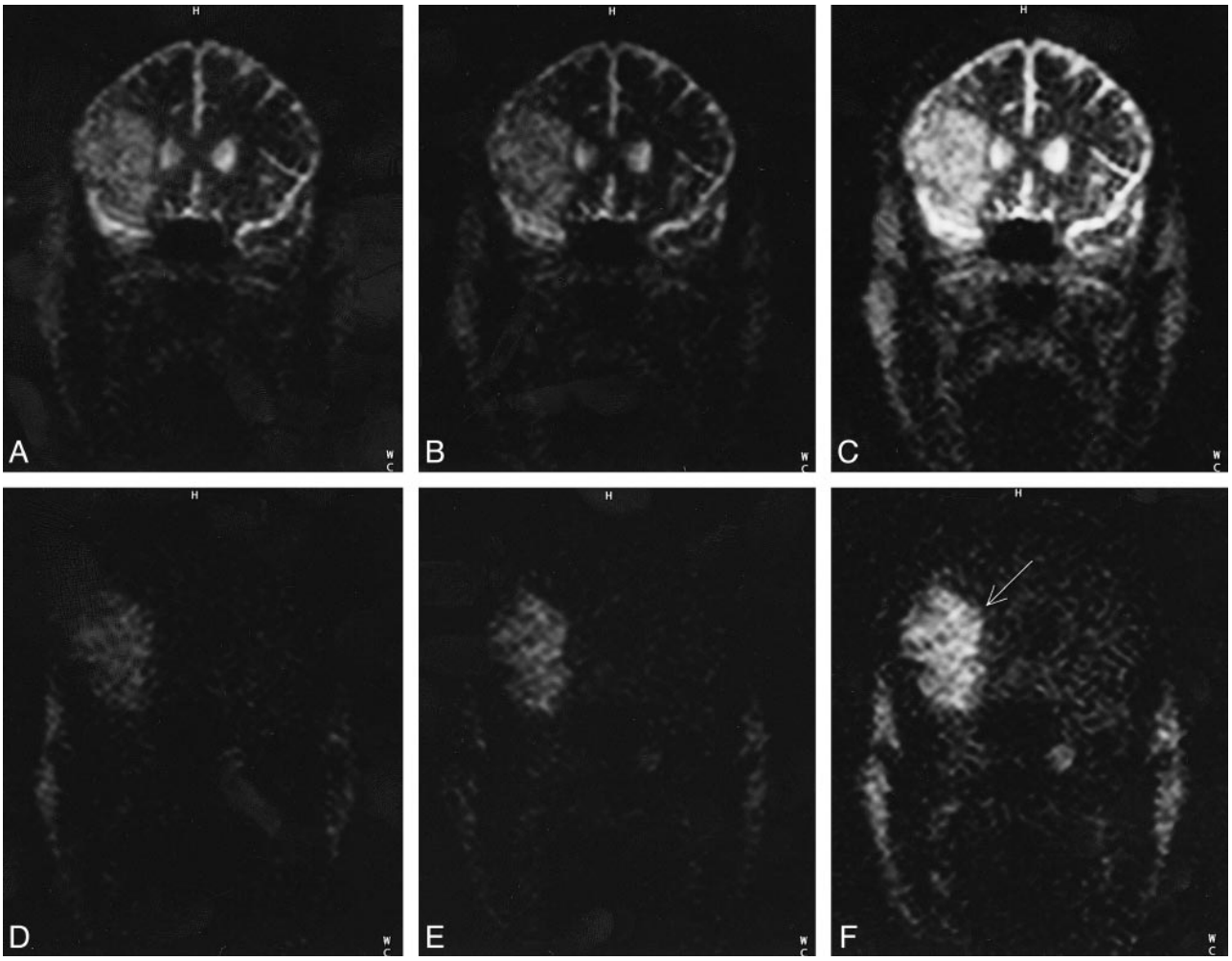

FIG 4. Effect of the addition of two separate magnitude images from echoes E1 and E2 in the modified fast spin-echo train in Figure 1A. Coronal single-shot images from a 74-year-old patient with a large ischemic lesion (*arrow, F*) were recorded using the half-Fourier approach. Section thickness, 12 mm; FOV, 175 × 350 mm; matrix, 96 × 256.

A–C, TE = 155; no diffusion sensitivity.

D–F, TE = 155; diffusion preparation with a *b* value of 1000 s/mm^2.

A and *D* are images from echoes E1; *B* and *E* are images from echoes E2; *C* and *F* are the addition of images from E1 and E2. Signal intensity is doubled, whereas noise increases by a factor of $\sqrt{2}$. CNR of the lesion versus normal brain is 11 in *F.*

brain lesions. The rationale for the development of this technique was that diffusion preparation and normal fast spin-echo acquisition do not work together. Phase shifts of the transverse magnetization after diffusion preparation are generated in case of linear motion, which is unavoidable in vivo. These undesired phase shifts result in negative interference of different signal pathways in normal fast spin-echo trains and consequently in dark subregions in diffusion-weighted standard fast spin-echo images. A prolongation of the readout interval in fast spin-echo sequences allows separation into two echo families (15). In a recently published article (16) it was reported that SPLICE recording of each of these echo families results in a complete image without sensitivity to the phase of the magnetization. Thus, even single-shot diffusion-weighted fast spin-echo imaging can be realized using adapted sequences with SPLICE data recording. In contrast to the original SPLICE sequence reported by these authors (16), a spin-echo diffusion preparation was used instead of a stimulated echo, because the signal yield from lesions with relatively long T2 is superior. In addition, the readout time for each echo in the echo train was longer (2.56 msec) for the measurements on the open system, as compared with 1.53 msec in the reported application on a high-field system.

A similar approach was shown by Alsop (17), but his technique uses only a part of the generated transverse magnetization and therefore provides lower signal intensity. Line scan diffusion imaging (19) is also a potential candidate for low-field applications; however, the minimum measuring time for one section is clearly longer, especially for high diffusion weighting.

The new methods with SPLICE allow an acceptable compromise between maximum SNR in the images, with long readout times required for species with long T2, and minimal problems with blurring of the signals, where a short refocusing

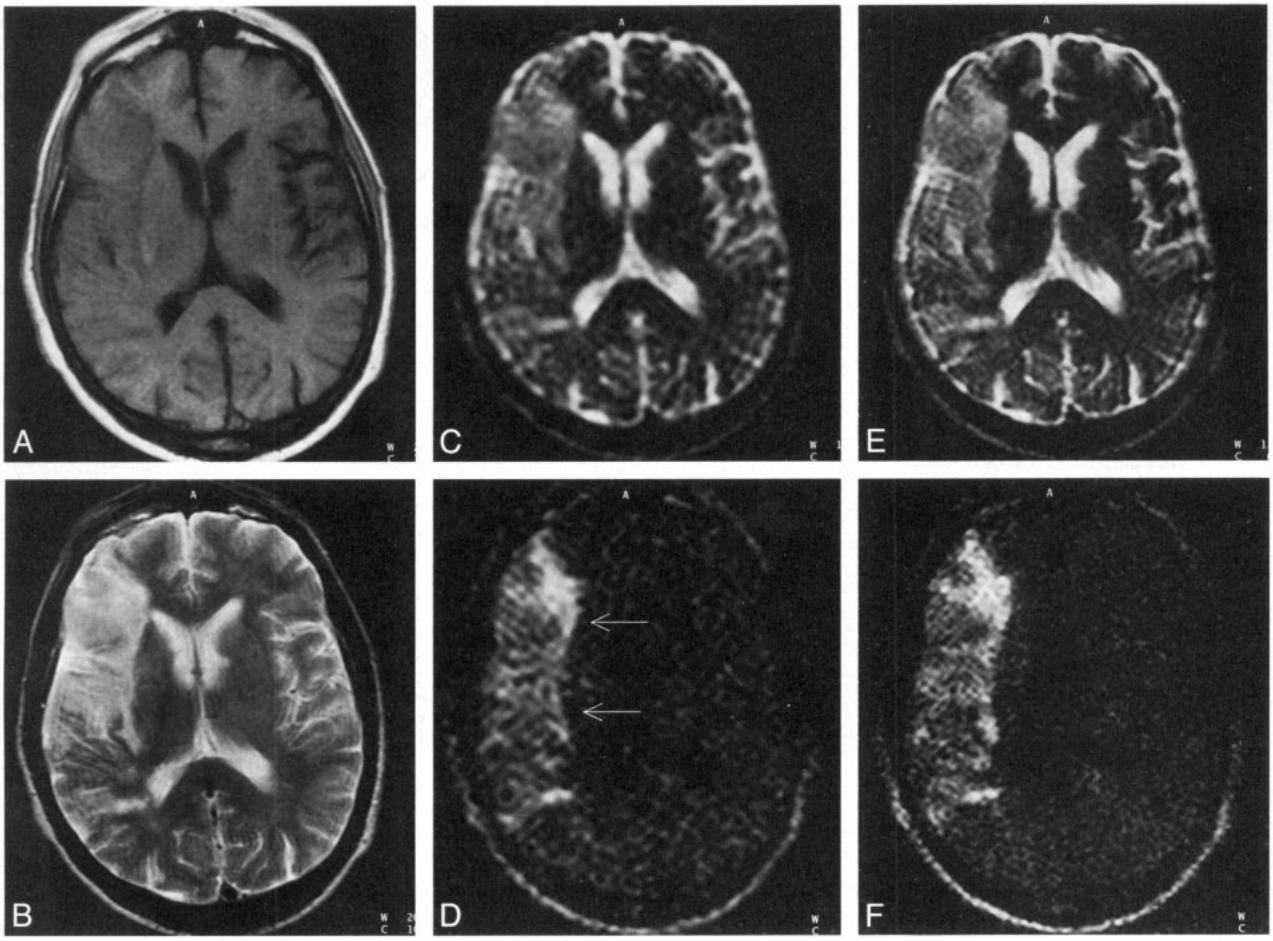

FIG 5. Transverse images from one section of the brain of a 74-year-old patient with occlusion of the middle cerebral artery, 10 days after onset of stroke symptoms.

A, Standard T1-weighted fast spin-echo image (400/15/2 [TR/TE/excitations]).

B, Standard T2-weighted fast spin-echo image (4000/117/1).

C, Single-scan half-Fourier image. Section thickness, 12 mm; FOV, 250 × 500 mm; matrix, 96 × 256; TE = 155; no diffusion sensitivity.

D, Single-scan half-Fourier image. Section thickness, 12 mm; FOV, 250 × 500 mm; matrix, 96 × 256; TE = 155; diffusion preparation with a *b* value of 1000 s/mm^2. CNR of the lesion (*arrows*) versus normal brain is 12.

E, Ten single-scan images from a set of 20 images were averaged. Half-Fourier approach, section thickness, 10 mm; FOV, 175 × 350 mm; matrix, 96 × 256; TE = 155; no diffusion sensitivity.

F, Ten single-scan images from a set of 20 images were averaged. Half-Fourier approach, section thickness, 12 mm; FOV, 250 × 500 mm; matrix, 96 × 256; TE = 155; diffusion preparation with a *b* value of 1000 s/mm^2. CNR of the lesion versus normal brain is 13.

period in the SPLICE acquisition train is required for species with short T2. Both half-Fourier acquisition and reordered phase encoding with recording of the entire k-space provided successful strategies. Averaging of several magnitude images from each section leads to improved results and allows smaller FOVs. In restless subjects, it has proved to be advantageous to select only scans recorded in a period without marked movement for signal averaging. However, each single image recorded in less than 1 s is relatively unaffected by motion, and ECG-triggering is unnecessary. The possibility of selecting suitable single scans for signal averaging after the examination seems to confer an important advantage over other techniques, which suffer from a marked loss in image quality in case of movement during acquisition. On the other hand, averaging is optional using these new methods.

Former approaches to subsecond diffusion-weighted imaging have failed to yield diagnostic results on open MR scanners. EPI (11) is too sensitive to unavoidable inhomogeneities of the static magnetic field, and it requires very fast gradient systems. Other methods based on small flip angle refocusing (15) and stimulated echoes (20, 21) provide lower SNR compared with the SPLICE acquisition train, since only parts of the maximum transverse magnetization are used. Standard fast spin-echo recording (22) was found to be quite sensitive to unavoidable motion. Thus, the new techniques provide interesting tools for MR imaging and for monitoring patients with ischemic lesions on open MR scanners. This type of MR unit allows good access to patients.

Low-field open MR systems usually allow only moderate slew rates and amplitudes of the field gra-

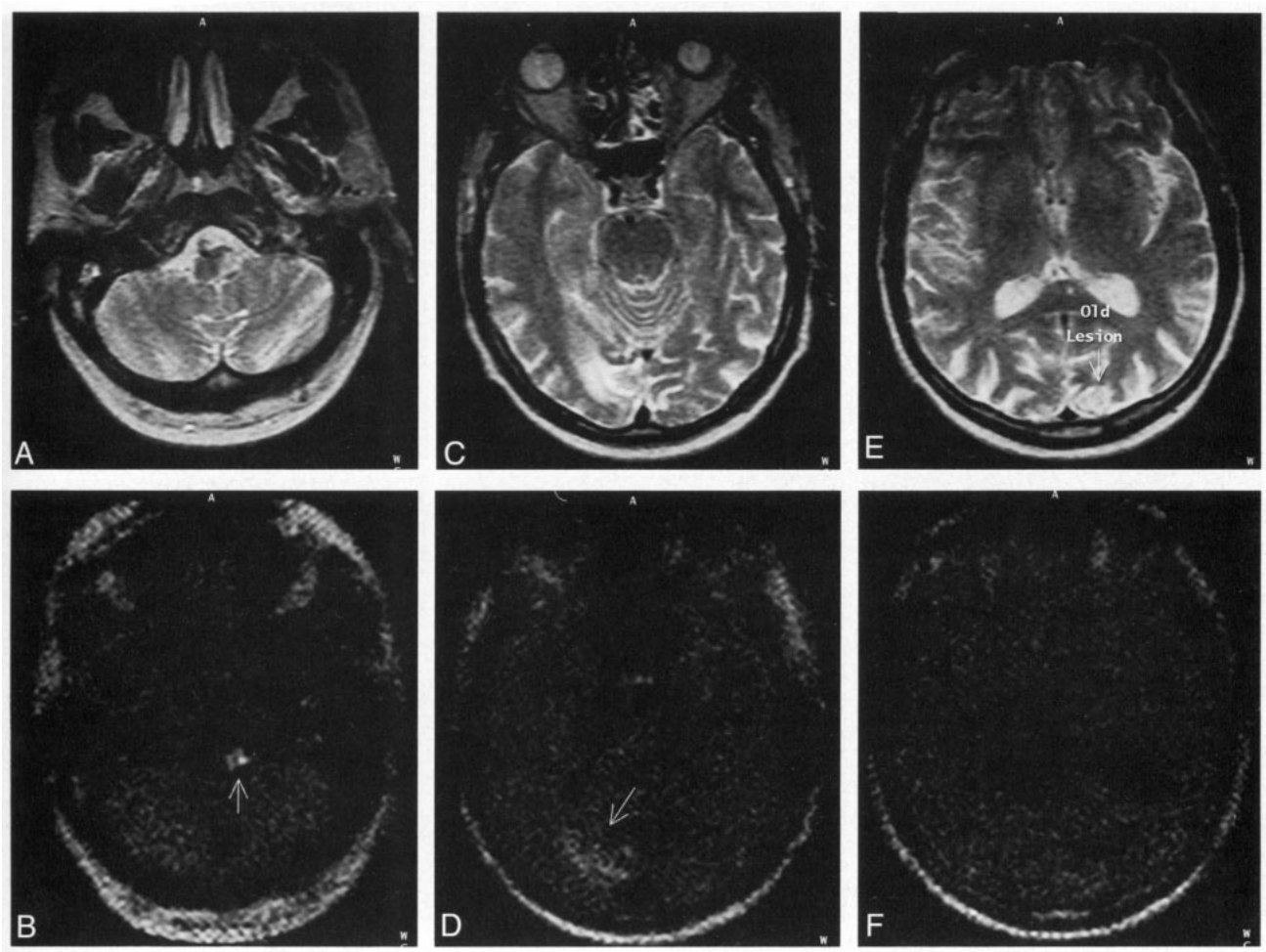

FIG 6. Clinical diffusion imaging in a 58-year-old patient with ischemic brain insults of different ages.

A, C, E, Anatomic details are well depicted on T2-weighted standard fast spin-echo images (4000/106/1).

B, D, F, Images show averaged signals from six single-shot scans with half-Fourier reconstruction. Diffusion-weighting (b = 1000 s/mm^2, TE = 155) allows distinction between the relatively recent lesion (6 days old, with markedly restricted diffusion (CNR = 10; *arrow, B*), the older lesion (4 weeks old) with slight signal enhancement (CNR = 4; *arrow, D*), and the 1-year-old lesion without any visible diffusion abnormalities. FOV, 175 × 350 mm; matrix, 96 × 256; section thickness, 10 mm.

dients. Therefore, relatively long diffusion preparation times must be accepted. The minimal TE is about 150 msec for diffusion weighting with b = 1000 s/mm^2 on the open 0.2-T imager. There are cases with changed diffusion properties in brain lesions that show relatively fast transverse relaxation, especially in the early phase of ischemia. Those cases lack prominent areas in the markedly T2-weighted images recorded without diffusion preparation. Consequently, signs of diffusion abnormalities are absent in the diffusion-weighted images, which are markedly T2-weighted as well. This problem occurs with open systems as well as with closed MR tubes possessing limited capabilities of the gradient system. It would be generally helpful to increase the maximum gradient amplitudes, but not necessarily the slew rates, to realize short TEs and high diffusion weighting at the same time. If these features are implemented in the next generation of open MR systems, the techniques presented here for fast diffusion-weighted imaging could be further improved and applied in patients with unclear cerebral lesions as well as in other types of tissue with faster transverse relaxation.

Acknowledgments

The members of Siemens Medizintechnik are acknowledged for continuous support. Beverly J. Geist-Barth carefully helped with manuscript revisions.

References

1. Moseley M, Cohen Y, Mintorovitch J, et al. **Early detection of regional cerebral ischemia in cats: comparison of diffusion- and T2-weighted MRI and spectroscopy.** *Magn Reson Med* 1990;14:330–346
2. Norris DG, Niendorf T, Hoehn-Berlage M, et al. **The incidence of apparent restricted diffusion in three different models of cerebral infarction.** *Magn Reson Imaging* 1994;12:1175–1182
3. Hoehn-Berlage M, Eis M, Back T, Kohno K, Yamashita K. **Changes of relaxation times (T1, T2) and apparent diffusion coefficient after permanent middle cerebral artery occlusion in the rat: temporal evolution, regional extent, and comparison with histology.** *Magn Reson Med* 1995;34:824–834
4. Le Bihan D, Breton E, Lallemand D, Grenier P, Cabanis E, Lavel-Jeantet M. **MR imaging of intravoxel incoherent motions: ap-**

plication to diffusion and perfusion in neurologic disorders. *Radiology* 1986;161:401–407
5. Warach S, Chien D, Li W, Ronthal M, Edelman RR. **Fast magnetic resonance diffusion-weighted imaging of acute human stroke.** *Neurology* 1992;42:1717–1723
6. Crespigny AJ, Marks MP, Enzmann DR, Moseley ME. **Navigated diffusion imaging of normal and ischemic human brain.** *Magn Reson Med* 1995;33:720–728
7. Warach S, Gaa J, Siewert B, Wielopolski P, Edelman RR. **Acute human stroke studied by whole brain echo-planar diffusion-weighted magnetic resonance imaging.** *Ann Neurol* 1995;37: 231–241
8. Ordidge R, Helpern JA, Qing ZX, Knight RA, Nagesh V. **Correction of motional artifacts in diffusion-weighted MR images using navigator echoes.** *Magn Reson Imaging* 1994;12:455–460
9. Anderson A, Gore J. **Analysis and correction of motion artifacts in diffusion-weighted imaging.** *Magn Reson Med* 1994;32:379–387
10. Müller MF, Prasad PV, Siewert B, Nissenbaum MA, Raptopoulos V, Edelman RR. **Abdominal diffusion mapping with use of a whole-body echo-planar system.** *Radiology* 1994;190:475–478
11. Mansfield P. **Multi-planar image formation by using NMR spin-echoes** (letter). *J Phys C* 1977;10:55–58
12. Haselgrove JC, Moore JR. **Correction for distortion of echo-planar images used to calculate the apparent diffusion coefficient.** *Magn Reson Med* 1996;36:960–964
13. Stejskal EO, Tanner JE. **Spin diffusion measurements: spin echoes in the presence of a time dependent field gradient.** *J Chem Phys* 1965;42:288–292
14. Hennig J, Nauerth A, Friedburg H. **RARE imaging: a fast imaging method for clinical MR.** *Magn Reson Med* 1986;3:823–833
15. Norris DG, Börnert P, Reese T, Leibfritz D. **On the application of ultra-fast RARE experiments.** *Magn Reson Med* 1992;27: 142–164
16. Schick F. **SPLICE: sub-second diffusion sensitive MR imaging using a modified fast spin-echo acquisition mode.** *Magn Reson Med* 1997;38:638–644
17. Alsop DC. **Phase insensitive preparation of single-shot RARE: applications to diffusion imaging in humans.** *Magn Reson Med* 1997;38:527–533
18. McGibney G, Smith MR, Nichols ST, Crawley A. **Quantitative evaluation of several partial Fourier reconstruction algorithms used in MRI.** *Magn Reson Med* 1993;30:51–59
19. Gudbjartsson H, Maier SE, Mulkern RV, Morocz IA, Patz S, Jolesz FA. **Line scan diffusion imaging.** *Magn Reson Med* 1996; 36:509–519
20. Merboldt KD, Hänicke W, Bruhn H, Gyngell ML, Frahm J. **Diffusion imaging of the human brain in vivo using high-speed STEAM MRI.** *Magn Reson Med* 1992;23:179–192
21. Yongbi MN, Ding S, Dunn JF. **A modified sub-second fast-STEAM sequence incorporating bipolar gradients for in vivo diffusion imaging.** *Magn Reson Med* 1996;35:911–916
22. Beaulieu CF, Zhou X, Cofer GP, Johnson GA. **Diffusion-weighted MR microscopy with fast spin-echo.** *Magn Reson Med* 1993;30: 201–206